Research Article

SULFIDE BASED PHOSPHOR OF Eu^{2+} DOPED STRONTIUM SULFIDE AND Ce^{3+} AND Bi^{3+} DOPED CALCIUM SULFIDE PHOSPHOR FOR SOLID STATE LIGHTING

*Maske B. R. [1], Moharil S. V.[1] and Bawankar R. D.[2]
[1]*Department of Physics, Rashtrasant Tukdoji Maharaj, Nagpur University, Nagpur (M.S), India*
[2]*Agnihotri College of Pharmacy, BapujiWadi, Wardha, (M.S), India*
*Author for Correspondence

ABSTRACT
Present investigation deals with sulfide based phosphor Eu^{2+} doped strontium sulfide and Ce^{3+} and Bi^{3+} doped calcium sulfide phosphor for solid state lighting. An attempt has been made to synthesize the phosphors (chosen material to synthesize such phosphors are strontium sulfide and Calcium sulfide act as host), which can be excited in the blue/ near UV region i.e. between the range 360 nm to 390 nm and emits in the red, green or blue region. SrSO$_4$: Eu phosphors, CaS: Ce phosphors and CaS: Biphosphors were prepared by recrystallization through sulfuric acid (Yamashita's method). Photoluminescence spectra were successfully recorded over Hitachi F-7000 fluorescence spectrophotometer in the range 220-700 nm. Results from SrS: Eu^{2+} showed intense red emission; intense green emission from CaS: Ce^{3+} whereas CaS: Bi^{3+} exhibits intense blue emission and thus helps in achieving safe disposal of burnt lamps causing minimization of environmental pollution, reduced by heating in reducing atmosphere provided by burning charcoal, minimization of stability problem (usually found under Hg discharge), solving problem of importing of phosphors by our country as we have developed reliable method for the synthesis of phosphorsuseful for solid state lighting.

Keywords: Solid State Lighting, Fluorescence, Luminescence, Strontium Sulfide, Calcium Sulfide, Phosphor

INTRODUCTION
Luminescence is the general term that covers both fluorescence and phosphorescence. The concept of fluorescence originated from the mineral fluorite because the phenomenon of light emission under ultraviolet radiation was first recognized in that mineral. Phosphorescence named after the well-known optical property of element phosphorous (Lakshmanan, 2008). In Greek, the term 'phosphor' means 'light bearer'. But the chemical element phosphorous is not phosphor. The difference between fluorescence and phosphorescence is to some extent arbitrary.

The increasing demand for fossil fuels and the environmental impact of their use are continuing to exert pressure on an already stretched World energy infrastructure (Zhang *et al.,* 2009). Conventional incandescent and fluorescent lamps rely on either heat or discharge of gases. Both phenomena are associated with large energy losses that occur because of the high temperatures and large Stokes shifts involved (Xie and Hirosaki, 2007). In 1996, Nichia Chemical Co. invented a totally new lighting device by means of a blue InGaN LED chip coated with yttrium aluminum garnet yellow phosphor (YAG:Ce) (Fasol and Nakamura, 2000). To give proper energy dispersion in the visible region, co-doping activators are required for single-phased white emitting phosphors such as Eu^{2+}Mn^{2+}and Ce^{3+}Mn^{2+} (Guo *et al.,* 2008). On the other hand, phosphors have been considered as key and technologically important components of the functionality and success of many lighting and display systems over the past several years. At present, rare-earth (RE)-based phosphors with efficiencies close to the theoretical maximum (100%) are employed in different fluorescent tubes, X-ray imaging, and color televisions. Such applications depend on the luminescent properties of RE ions, e.g. sharp lines, high efficiency, and high lumen equivalence (Zhang and Huang, 2010). However, a good phosphor for electronic or X-ray excitation is not necessarily a good choice for excitation by semiconductor LED chips. Most previously indentified phosphors for general illumination have been developed for Hg discharge lamps (fluorescent

Research Article

lamps), which are designed to fit the excitation of 254 nm (low-pressure Hg lamps) or 365 nm (high-pressure Hg lamps) UV light. By far, most of the commercial phosphors for lighting are oxide-based materials, and only a few of them can be excited efficiently by blue InGaN chip (λex = 420–480 nm), such as YAG: Ce and other garnet phosphors (Wu *et al.,* 2007). Additionally, the temperature-quenching of YAG: Ce is a big challenge for white LED applications. Accordingly, a new hot topic of nitride and oxynitride phosphors has recently attracted much attention (Li *et al.,* 2005; Li *et al.,* 2007). Commercial phosphors for white UV-LED applications (λex = 365–410 nm) are also scarce, especially red phosphors. Much effort has been dedicated to the phosphors in pc-WLEDs, which could be excited efficiently by blueor NUV lights. RE ions and transition metal (TM) ions are the most frequently used phosphor activators (Wang *et al.,* 2005; Ye *et al.,* 2009).

Luminescence is defined as the emission of electromagnetic radiation in excess of thermal radiation (Blasse and Grabmeier, 1994). Luminescence differs from incandescence, which is a process in which solids emit light by reason of their high temperatures (Hill, 1984). The electronegativity of S is smaller than that of O, and S could be polarized easily. Thus, the nephelauxetic effect in sulfides is generally larger than that in oxide-based compounds, which results in large centroid shift of Ce^{3+} or Eu^{2+} (Dorenbos, 2003). The Ce^{3+} and Eu^{2+} in alkaline earth sulfides can absorb blue light and give green to red light emission gives the spectra of alkaline earth sulfide phosphors excited by 450 nm blue-LED chips.

Very little work has been done in India on development of phosphor for solid state lighting. It is likely that our country will go for large scale import of such phosphors during next decades and so need arise to develop our own phosphors. Hence, we have to synthesize the phosphors, which can be excited in the blue/ near UV region i.e. between the range 360 nm to 390 nm and emits in the Red, Green or Blue region. Present investigation was aimed to choose Strontium sulfide and Calcium sulfide as a host to synthesize such phosphors which act as good luminescence materials. The problem of stability under Hg discharge occurred as excitation spectra of several sulfides did not overlap with Hg 253.7 nm line.

Experimental
Re-crystallisation Method
Samples were prepared by dissolving desired quantities of strontium nitrate in doubled distilled water and Eu_2O_3 in conc, HNO_3 stirred it well till we get clear solutions. These above solutions were mixed together. Conc. sulphuric acid was then added to this solution in excess quantity. All solutions were taken into the three necked conical flasks for processing acid distillation. Strontium sulphate doped with europium was obtained in white crystalline powder form. Washed the sample by double distilled water and dried it. Dried samples were annealed for 4 hours at 850^0C in a reducing atmosphere provided by burning charcoal so as to convert sulphate into sulfide and activators reduced to divalent state. The annealed powder were sandwiched between quartz plates and transferred to photoluminescence cell. Photoluminescence spectra were recorded in the range 220-700 nm on Hitachi F-7000 spectra-fluorimeter with spectral slit width of 1.5 nm.

Measurement of the Excitation and Emission Spectra
A powder sample cell (consists of quartz disc) was used to record the photoluminescence spectra. The quartz disc was fixed into the sample holder and powder sample was spread on it. Then, the threaded cap was fitted to hold the powder sample. The metal frame was put on the sample cell, containing sample so that the front protrusion of the cell could fit into the metal frame aperture. When analyzing the sample, optical axis will run along the centre line of powder surface (quartz window).

First the excitation (EX) spectra were recorded by setting the emission wavelength at zero order and keeping other parameters as specified in the manual. The excitation bands (EX) were identified from these spectra and the emission (EM) spectra were scanned for identified excitation wavelengths.

It was necessary to know approximate nature of EX and EM spectra. While doing so the direct scattered light may superimpose on the EX spectrum, so, it is necessary to select a particular band in the emission for scanning the EX. Therefore, for proper excitation wavelengths EM was set at the position as identified from the earlier emission spectrum. Again the same procedure was followed for identifying correct EX positions and EM was recorded for each EX band separately.

Research Article

In the ordinary measurements, a spectrum is affected by wavelength characteristics of the analysis system (monochromator, photomultiplier etc.). In order to measure a spectrum correction was performed using Rhodamine B as a standard. Similarly, emission spectrum was corrected by using diffuser and attenuator mentioned in the instrument manual. Both the spectra were correctable in the range of 220 to 600 nm. The sample whose emission wavelengths were within 220 to 600 nm were scanned in the correct spectrum mode and the samples whose wavelengths were beyond 600 nm were scanned in ordinary mode.

Emission spectra were recorded with excitation band pass 5 nm and emission band pass 1.5 nm, while the excitation spectra were recorded with excitation band pass of 1.5 nm and emission band pass 5 nm.

Same procedure was adopted for Cerium and Bismuth doped Calcium Sulfide phosphors.

Specification of Hitachi F-7000:

Light Sours	150 W Xelamp, with self-deozonating lamp house.
Monochromatometer	Provided on both excitation and emition sides Large-bore aberration-free concave diffraction gratin g of 900 lines/mm. Blaze wavelength; EX side 30nm, EM side 400nm.
Wavelength range	200 to 700 nm and 0-order light on both EX and EM sides (wavelength indication 200 to 900 nm and 0-order light)
Sensitivity	S/N 250 or more (peak–to-peak), S/N 800 or more (RMS) upon measuring Raman spectrum of water. Ex wavelength : 350 nm Slit (both EX and EM) : 5 nm Response : 2 s
Wavelength accuracy	Within ±1.0 nm
Wavelength scan speeds	30, 60, 240, 1200, 2400, 12000, 30000, 60000nm/min
Wavelength drive speeds	60000 m/min
Slits	EX side : 1.0, 2.5, 10, 20 nmEM side : 1.0, 2.5, 10, 20 nm
Resolution	1.0 nm(using Hg bright line at 546.1 nm)
Response speed	For 98% response:0.002, 0.004, 0.01, 0.05, 0.1,0.5,2,4,8 sec.
Photometric range	-9999 to 9999
Photometric system	Monochromatic light monitoring ratio photometry
Minimum sample volume	0.6 mL (using standard 10 mm rectangular cell)
Communication function	USB communication
Dimensions (spectrometer main unit)	620 width x 520 depth x 300 height (mm)
Weight (spectrometer main unit)	Approx. 41 Kg
Power supply voltage (spectrometer main unit)	100, 115, 220, 230, 240 V AC, 50/60 Hz
Power consumption (spectrometer main unit)	380 VA

Synthesis

As described in the experimental section, in the first step, $SrSO_4$: Eu phosphors were synthesized by recrystallization through sulfuric acid (Yamashita's method). Reduction to SrS was achieved by heating

Research Article

this phosphor in reducing atmosphere provided by burning charcoal. Figure 3.1 shows comparison of XRD pattern for SrS so prepared. For the thermal treatment of 900 C, 2 hours in the reducing atmosphere, SrS was effectively formed as can be seen from the comparison of recorded diffraction pattern with ICDD file 75-0895. However, there are some extra lines present in the pattern which can be identified with $SrSO_4$ (ICDD 89-0954). When the reduction was carried out at 850 C for 4 hours, the extra lines almost disappeared. Thus, the simple method described in the experimental section is adequate for converting $SrSO_4$ to SrS. Similarly, CaS: Ce and CaS: Bi were prepared by above same method.

Calculations

Calculation of SrS:Eu

SrS:Eu (0.1 mol%)

 Molecular weight of $Sr(NO_3)_2$=211.63 a.m.u   Molecular weight of Eu_2O_3 =351.98 a.m.u

 Molecular weight of H_2SO_4 =98.08 a.m.u

$(0.999 * Sr(NO_3)_2 + (0.001* 0.5 * EuO_3) + Conc. H_2SO_4$

$(0.999 * 211.63+ (0.0005 * 351.98) + 1$ mol of 98.08

$211.41837 + 0.17599 + 98.08$

Take $Sr(NO_3)_2 = 4$ g.

We take $Eu_2O_3 = \frac{0.17599*4}{211.41837}$ = 0.0033 g.

Conc.H_2SO_4 $=\frac{(^{98.08}/_{211.41837})}{1.8032}$ $* 4$ =1.29091 ml.

Take excess four times i.e. 4.116364 ml.≈ 5 ml.

SrS:Eu (0.2 mol%)

Molecular weight of $Sr(NO_3)_2$=211.63 a.m.u   Molecular weight of Eu_2O_3 =351.98 a.m.u

Molecular weight of H_2SO_4 =98.08 a.m.u

$(0.998 * Sr(NO_3)_2 + (0.002 * 0.5 * EuO_3) + Conc. H_2SO_4$

$(0.998 * 211.63+ (0.001 * 351.98) + 1$ mol of 98.08

$211.20674 + 0.35198 + 98.08$

Take $Sr(NO_3)_2 = 4$ g.

We take $Eu_2O_3 = \frac{0.35198 *4}{211.20674}$ = 0.0067 g. Conc.H_2SO_4 $=\frac{(^{98.08}/_{211.20674})}{1.8032}$ $* 4$ =1.030122 ml.

Take excess four times i.e. 4.1204890 ml.≈ 5 ml. The procedure was the same as that of above.

SrS:Eu (0.5 mol%)

$(0.995 * Sr(NO_3)_2 + (0.005 * 0.5 * EuO_3) + Conc. H_2SO_4$

$(0.995 * 211.63+ (0.0025 * 351.98) + 1$ mol of 98.08

$210.57185 + 0.87995 + 98.08$

Take $Sr(NO_3)_2 = 4$ g.

We take $Eu_2O_3 = \frac{0.87995 *4}{210.57185}$ = 0.0167 g.

Conc.H_2SO_4 $=\frac{(^{98.08}/_{210.57185})}{1.8032}$ $* 4$ =1.03322 ml.

Take excess four times i.e. 4.132912 ml.≈ 5 ml.

The procedure was the same as that of above.

SrS:Eu (1 mol%)

$(0.99 * Sr(NO_3)_2 + (0.01* 0.5 * EuO_3) + Conc. H_2SO_4$

$(0.99 * 211.63+ (0.005 * 351.98) + 1$ mol of 98.08

$209.5137 + 1.7599 + 98.08$

Take $Sr(NO_3)_2 = 4$ g.

We take $Eu_2O_3 =\frac{1.7599 * 4}{209.5137}$ = 0.034 g.

Conc.H_2SO_4 $=\frac{(^{98.08}/_{209.5137})}{1.8032}$ $* 4$ =1.038446 ml.

Research Article

Take excess four times i.e. 4.1537859 ml.≈ 5 ml. The procedure was the same as that of above.

For calculation of CaS:Ce,

CaS:Ce (0.1 mol %)

Molecular weight of $CaCO_3$=100.09 a.m.u   Molecular weight of $Ce_2(SO_4)_3$ =568.43 a.m.u

Molecular weight of H_2SO_4 =98.08 a.m.u

$(0.999 * CaCO_3 + (0.001* 0.5 * EuO_3) + Conc. H_2SO_4$

$(0.999 * 100.09 + (0.0005 * 568.43) + 1$ mol of 98.08

99.9899 + 0.2842+ 98.08

Take CaCO3= 2 g.

We take $Ce_2 (SO_4)_3$= (0.2842*2)/99.9899 = 0.0057g.

Take Stock solution, 0.5g = 10 ml.

$Ce_2 (SO_4)_3$ = 0.0057/0.5 =0.1136 ml.Conc.H_2SO_4= (98.08/99.9899)*2/1.8032=1.08784ml.

Take excess four times i.e. 4.3513 ml.≈ 5 ml.

CaS:Ce (0.2 mol %)

Molecular weight of $CaCO_3$=100.09 a.m.u   Molecular weight of $Ce_2 (SO_4)_3$ =568.43 a.m.u

Molecular weight of H_2SO_4 =98.08 a.m.u

$(0.998 * CaCO_3 + (0.002* 0.5 * EuO_3) + Conc. H_2SO_4$

$(0.998 * 100.09 + (0.002 *0.5* 568.43) + 1$ mol of 98.08

99.8899 + 0.56843+ 98.08

Take CaCO3= 2 g.

We take $Ce_2 (SO_4)_3$ = (0.56843*2)/99.8899 = 0.011 g.

Take Stock solution, 0.5g = 10 ml. $Ce_2 (SO_4)_3$= 0.011/0.5 =0.023 ml.

Conc.H_2SO_4= (98.08/99.8899)*2 /1.8032=1.08906 ml.

Take excess four times i.e. 4.35624 ml.≈ 5 ml.

CaS:Ce (0.5 mol %)

Molecular weight of $CaCO_3$=100.09 a.m.u   Molecular weight of $Ce_2 (SO_4)_3$ =568.43 a.m.u

Molecular weight of H_2SO_4 =98.08 a.m.u

$(0.995 * CaCO_3 + (0.005* 0.5 * EuO_3) + Conc. H_2SO_4$

$(0.995 * 100.09 + (0.005 *0.5* 568.43) + 1$ mol of 98.08

99.58955 + 1.421075+ 98.08

Take CaCO3= 2 g.

We take $Ce_2 (SO_4)_3$ = (1.421075*2)/99.8899 = 0.029 g.

Take Stock solution, 0.5g = 10 ml.

$Ce_2 (SO_4)_3$= 0.029/0.5 =0.057 ml.

Conc.H_2SO_4= (98.08/99.58955)*2/1.8032=1.1.09232 ml.

Take excess four times i.e. 4.36928 ml.≈ 5 ml.

For calculation of CaS:Bi

CaS:Bi (0.1 mol %)

Molecular weight of $CaCO_3$=100.09 a.m.u   Molecular weight of $Bi (NO_3)_2 .H_2O$=485.07 a.m.u

Molecular weight of H_2SO_4 =98.08 a.m.u

$(0.999 * CaCO_3 + (0.001*1*Bi(NO_3)_2 .H_2O) + Conc. H_2SO_4$

$(0.999 * 100.09 + (0.001*485.07) + 1$ mol of 98.08

99.9899 + 0.48507+ 98.08

Take CaCO3= 3 g.

We take $Bi(NO_3)_2 .H_2O$ = (0.48507*3)/99.9899=0.015 g.

Take Stock solution, 0.5g = 10 ml. $Ce_2(SO_4)_3$= 0.015/0.5 =0.2910 ml.

Conc.H_2SO_4= (98.08/99.9899)*3/1.8032=1.6317ml.

Excess amount was taken i.e. four times 6.5268ml.≈ 7 ml.

Research Article

RESULTS AND DISCUSSION
For SrS:Eu^{2+}

Eu^{3+}or Eu^{2+} can be identified from the characteristic photoluminescence they exhibit. Eu^{2+} emission arises from the lowest band of 4f^{6}5d^1 configuration to ^{8}S$_{7/2}$ state of 4f^7 configuration. The excitation arises from the transition from ^{8}S$_{7/2}$ state of 4f^7 configuration to the states belonging to 4f^{6}5d^1 configuration. Due to allowed nature of the transition, PL is intense. Spectral positions of these bands vary a great deal from lattice to lattice. f-f transitions of Eu^{3+}, on the other hand, are forbidden and Eu^{3+} PL is in general weak, unless there is excitation by charge transfer or energy transfer from a sensitizer. In general, narrow emission bands may be observed at about 570, 590, 610, 650 and 700 nm corresponding to transitions ^{5}D$_0$->^{7}F$_0$, ^{7}F$_1$, ^{7}F$_2$, ^{7}F$_3$, ^{7}F$_4$, respectively. Eu^{3+} emission usually occurs from ^{5}D$_0$→^{7}F$_j$ transitions. There are three transitions which are of prime importance ^{5}D$_0$→^{7}F$_0$(around 570 nm), ^{5}D$_0$→^{7}F$_1$(around 595 nm) and ^{5}D$_0$→^{7}F$_2$ (around 610 nm).

The first one is strongly forbidden transition and yet observed with appreciable intensity in some hosts. ^{5}D$_0$→^{7}F$_1$ transition is forbidden as electric dipole, but allowed as magnetic dipole. This is the only transition when Eu^{3+} occupies a site coinciding with a centre of symmetry. When Eu^{3+} ion is situated at a site, which lacks the inversion symmetry, then, the transitions corresponding to even values of j (except 0) are electric dipole allowed and red emission can be observed. ^{5}D$_0$→^{7}F$_1$ transition can also be observed as magnetic dipole allowed transition. Further, all the lines corresponding to these transitions split into number of components decided by the local symmetry.

Eu^{2+} emission arises from the lowest band of 4f^{6}5d^1 configuration to ^{8}S$_{7/2}$ state of 4f^7 configuration. The excitation arises from the transition from ^{8}S$_{7/2}$ state of 4f^7 configuration to the states belonging to 4f^{6}5d^1 configuration. The ground state electronic configuration of Eu^{2+} is 4f^7. This results in a ^{8}S$_{7/2}$ level for the ground state.

The next f^7 manifold (^{6}P$_j$) lies approximately 28000 cm-1 higher. The lowest lying 4f^{6}5d levels begin near 34000 cm^{-1} and are labeled ^{8}H$_J$ for the free ion. The 4f^{6}5d levels experience much more crystal field splitting than the 4f^7 levels due to the increased spatial extent of the 5d orbitals and often are the metastable state, or the lowest excited state, when the Eu^{2+} ion is incorporated in a crystalline host. The effect of the crystal field on the 5d electron is to split the 5d orbitals into two components t$_{2g}$ and e$_g$. The isotropic part of the exchange interaction between 5d and 4f electrons results in an exchange splitting into states with total spins of S= 7/2 and 5/2.

Thus, for the absorption spectra of Eu^{2+} in the solids, the lowest energy band arises from the state described by the notation |4f6 (7Fj)e$_g$, S=7/2>. The lowest energy configuration corresponds to the situation where ^{7}F$_J$ (4f$_6$) state couples to the 5d e$_g$ orbital such that all spins are parallel. Spectral positions of these bands vary a great deal from lattice to lattice. The most commonly observed emission is the dipole and spin allowed d-f-emission starting from the relaxed 4f^6(^{7}F$_0$) 5d^1 level (**Figure 1.2A**). Due to allowed nature of the transition, d-f emission is intense.

In some cases especially in certain fluorides, position of the band corresponding to f-d transition lies above f-f levels (Figure 1.2B). Line emission corresponding to ^{6}P$_j$→^{8}S$_{7/2}$ transitions of 4f^7 configuration is then observed. A third type of emission involving the Eu^{2+} ions is often characterized by a very large Stokes (5000 –10000 cm^{-1}) shift, very broad (>4000 cm^{-1}) emission bands, and deviating temperature behavior. This ''anomalous'' emission has been attributed to auto-ionization of the 5d electron to conduction band level (Figure 1.2 C). The electron is localized on the cations around the hole that stays behind on Eu^{2+}; and an impurity trapped excitation state is created. The ''anomalous ''emission is the radioactive transfer of the electron back to the ground state of Eu^{2+}. Auto-ionization can also be a cause for absence of Eu^{2+} luminescence.

Figure 1.2A (i) showed PL spectra for various samples. As prepared SrSO$_4$: Eu sample does not show any luminescence. Eu is not incorporated in divalent form and perhaps emission of Eu^{3+} is too weak to be observed. When SrSO$_4$: Eu is heated in air at 900 C, Eu gets incorporated in divalent form. A strong emission (curve a) is observed in form a well-defined band around 377 nm. This arises from the lowest band of 4f^{6}5d^1 configuration to ^{8}S$_{7/2}$ state of 4f^7 configuration. The excitation spectrum (curve b) contains

Research Article

several bands which correspond to transition from $^8S_{7/2}$ ground state to various states of $4f^65d^1$ configuration. For SrS: Eu, the position of the lowest band of $4f^65d^1$ configuration is well below the levels corresponding to $4f^7$ configuration. The excitation and emission, both are shifted to much longer positions as compared to $SrSO_4$: Eu. This can be attributed to strong electronegativity of S^{-2} as compared to that of oxygen ion. Emission peaks at about 601 nm. Excitation spectrum (curve d) is very broad extending from violet into the green region of the spectrum.

Figure 1.2A (i) shows PL spectra for various Eu concentrations. PL intensity increases with the concentration, reaching maximum value for 0.5 mol%. A decrease is observed for higher concentrations due to concentration quenching.

For CaS:Ce^{3+}

As all the PL results are related with Ce^{3+} activator, a brief discussion on PL of Ce is given below:

The 5d-level spectroscopy of Ce^{3+} is very simple. In the excited state, the 4f-shell is empty and there is only one single 5d-electron interacting with the crystalline environment. In the ground state, Ce^{3+} ion has the (Xe) $4f^1$ configuration, which results in only two $4f^1$ energy levels: the $^2F_{5/2}$ and $^2F_{7/2}$. These are the only level possible for 4f configuration. f-f transition of Ce^{3+} is in IR region. At room temperature, they occur as unresolved bands with maximum at about 2200-2300 cm^{-1} and half width 250-300 cm^{-1}. At low temperature the band splits into some lines which are due to f-f transition and electro vibronic transition (Mandel *et al.,* 1960; Kiss, 1962; Buchanan *et al.,* 1966).

At higher energy, the $4f^05d^1$ bands can be found. The excited states above $^2F_{7/2}$ level belong to 5d configuration in the form of bands. The energy of the bands is strongly dependent on the host lattice. The $4f^1$ ground state is separated about 51000 cm^{-1} from the excited $5d^1$ configuration. In a crystalline environment, the 5d configuration may split by as much as 25000 cm^{-1} into at most five distinct 5d states. In addition, the average energy of the five 5d-levels may shift downwards by 22000 cm^{-1}.

The red shift of the first f–d-transition in Ce^{3+} when introduced in a crystalline host is a result of two mutually independent contributions: (1) The centroid shift, defined as the lowering of the average energy of the Ce^{3+} 5d configuration relative to the value for Ce^{3+} as a free ion. (2) The total crystal field splitting; defined as the energy difference between lowest and highest 5d-level. A typical example of splitting of Ce^{3+} energy levels from ref (Wang *et al.,* 2006) is given in the Figure 1.2B. The 4f–5d transitions corresponding to optical absorption and fluorescence of Ce^{3+} in crystals are parity and spin-allowed so that lifetimes of the fluorescence are in the range of 10 – 60 ns. Ce^{3+} doped phosphors are thus useful where rapid decay times are required e.g. in time of flight camera and scintillators.

When Ce^{3+} ion is incorporated into the lattice the spatially diffuse 5d-electron orbital extends outward from the ion to overlap the neighbouring ligand ions, and is more strongly influenced by their motion. In consequence, the optical properties depend strongly on structure of host crystals. Most commonly observed emission is characteristic of 5d-4f transition. Both absorption and emission have a usually broad band character, showing splitting characteristic of ^2F_j states.

The Stokes shift is due to interaction with host crystal. As the position of 5d band itself depends on the host, not only the Stoke's shift but also the spectral positions of both the excitation and emission bands are host dependent. For example in Y_2SiO_5:Cethe emission is around 400nm while in $(Y)_3Al_5O_{12}$:Ce the Ce^{3+} emission is in the form of a very broad band stretching from 500 nm to well beyond 700 nm having maximum around 550 nm (Hoffman, 1977) and in sulphides such as CaS, Y_2O_2S it is in green- red region (Yokomo *et al.,* 1979; Kawai *et al.,* 1981). Emission at longer wavelength is obtained when the center of the 5d level is at relatively low energies (strong Nephelauxetic effect) and the crystal field is very strong.

Luminescence of Ce^{3+} gets quenched above concentration of about 5 % due to Ce^{3+}-Ce^{3+} transfer followed by transport to killer site.

The quenching temperature is usually high. Ce usually shows high quenching temperature in silicates, borates and phosphates. Since Ce^{3+} has a strong absorption in many hosts and emission matching with $4f^n$ levels of other rare earth impurities it can be used as a sensitizer for Tm^{3+}, Sm^{3+}, Dy^{3+}, Tb^{3+}, Nd^{3+}, Gd^{3+}, and Pr^{3+}. Ce^{3+} can also sensitize the luminescence in the host containing the transition metal activators like Mn.

Research Article
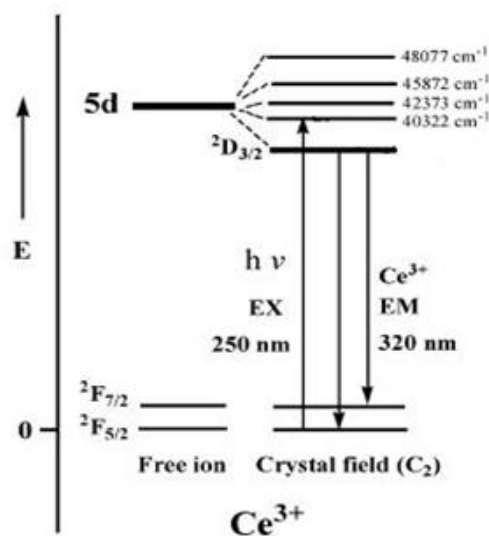
Figure 1.2B: A Typical Example of Crystal Field Splitting of 5d Energy Levels of Ce^{3+} Ion in CeF$_3$

Ce^{3+} exhibits intense emission due to allowed electric dipole transitions corresponding to transition from levels of 5d^1 configuration to 2f$_j$ states of 4f^1 configuration with fast decay time of the order of several nanoseconds. We have prepared Ce^{3+} activated sulfide based phosphors using Yamashita's method. Ce^{3+} emission was observed. Synthesis of phosphors and data on photoluminescence are presented in this work.

Photoluminescence (PL) of Ce3$^+$ (0.1%) activated CaS are presented in figure 1.2B (i). Intense emission was observed for 450nm, excitation is in the form of characteristics double peaks located at 243.75nm and 456.25nm.

Photoluminescence (PL) of Ce^{3+} (0.2%) activated CaS are presented in figure 1.2B (ii). Intense emission was observed for 450nm, excitation is in the form of characteristics double peaks located at 243.75nm and 456.25nm.

Photoluminescence (PL) of Ce^{3+} (0.5%) activated CaS are presented in figure 1.2B (iii). Intense emission was observed for 450nm, excitation is in the form of characteristics double peaks located at 250nm and 456.25nm.

ForCaS:Bi^{3+}

It is well known that the fluorescent properties of Bi^{3+} activated phosphors are generally due to electronic transitions of Bi^{3+}. As for other mercury –type ions, the configuration is 6S^2 in the ground state and 6s6p in the first excited state. Only ^{1}P$_1$ and ^{3}P$_1$, lead to allowed transitions ^{3}P$_2$ and ^{3}P$_0$ are metastable. The s2-sp transition of Bi^{3+} is an allowed one: Luminescence spectrum of ions with s2-sp transition such as Bi$^{3+,}$ Pb$^{2+,}$ Sn^{2+}, and Sb^{3+} shows a very broad gaussian band.

Bismuth activated CaS, CaS: Bi, has been well known for a long time as a blue phosphor and used as a photoluminescence, electroluminescence, cathode luminescence and thermoluminescence material. Figure 3.2C showed PL results for ns^2 activators in CaS.

Excitation Spectra of CaS:Bi.: Two peaks are observed in excitation band at about 306.25nm and 418.75nm. The shoulder may be due to aggregation of the activator into pairs. The ground state of Bi^{3+} with 6s2 configuration is 1S0. The excited levels have 6s6p configuration. Thus, 3P0, 3P1, 3P2, and 1P1 are possible states.

Figure 1.2C shows the energy levels of ns2 ion in the Oh symmetry. The transitions from 1S0 to 3P0 and 3P2 are completely spin forbidden, but the two levels 3P1 and 1P1 are mixed by spin-orbital coupling. Therefore, the transitions 1S0, 3P1and 1P1 are allowed transitions and are expected to have reasonable absorption intensity. The excitation spectra of CaS: Bi are shown in Figure 1.2C (i).
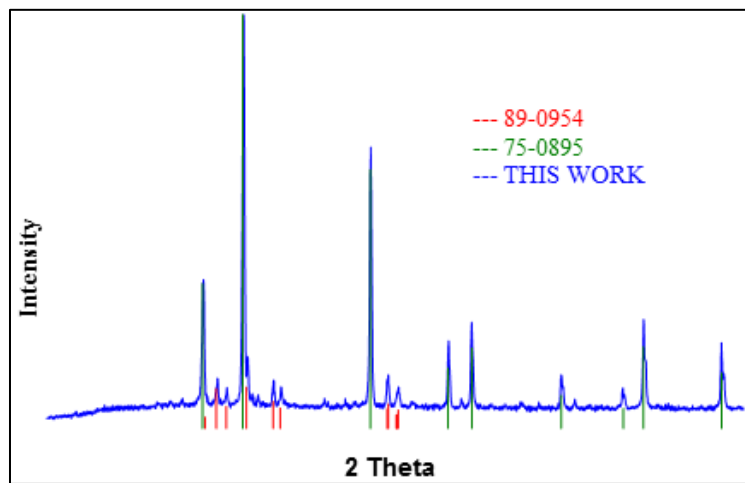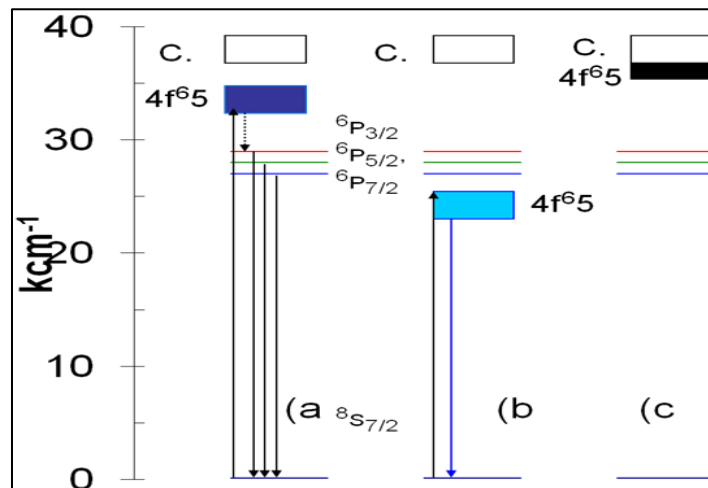
Research Article
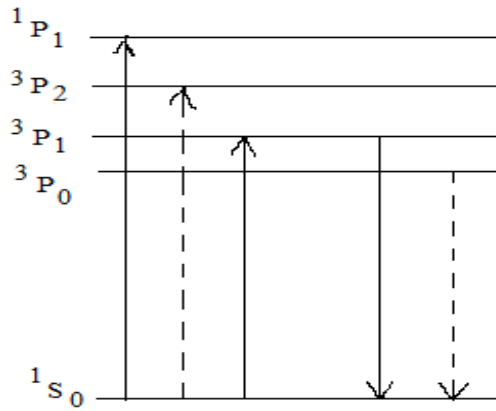
Figure 1.2C: Energy Level Diagram of a ns2 Ion(Bi) in the Oh Symmetry, Solid Lines are Allowed Transition and Dashed Lines are Forbidden Transitions

Emission Spectra of CaS:Bi: A emission band is observed around 448 nm for Bi^{3+} (0.1%) for 310 nm excitation see figure 1.2C(i).
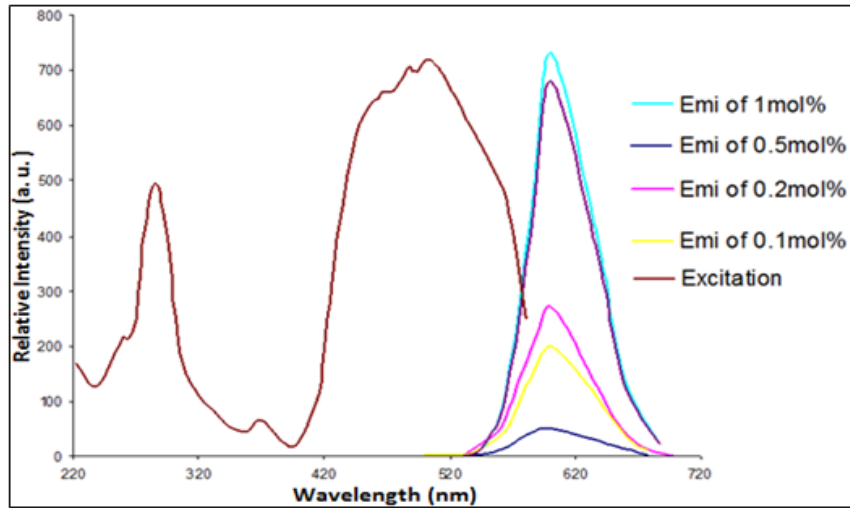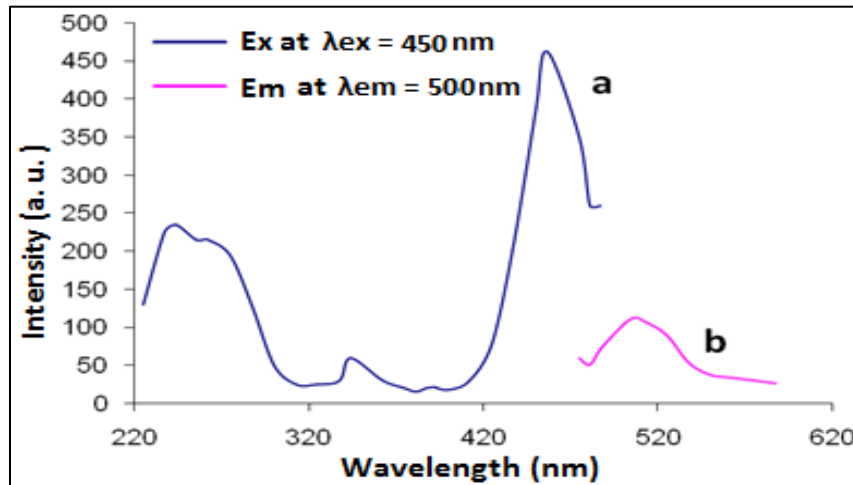

Figure 1.1:- XRD Pattern of SrS
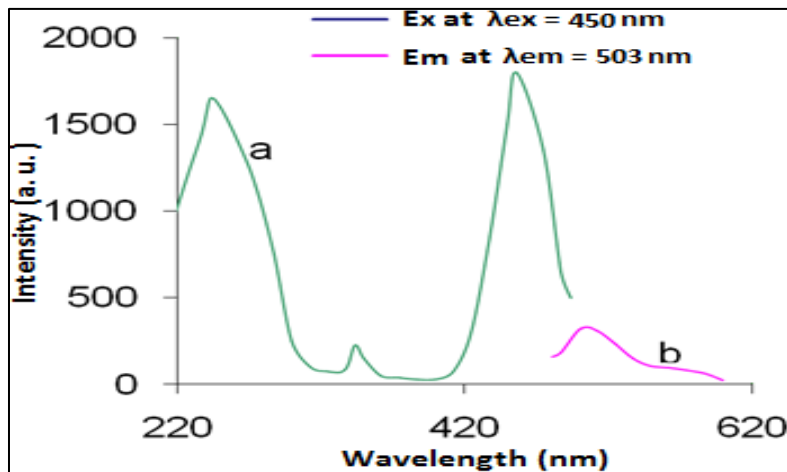

Figure 1.2: Transition of $Eu2^+$

Research Article

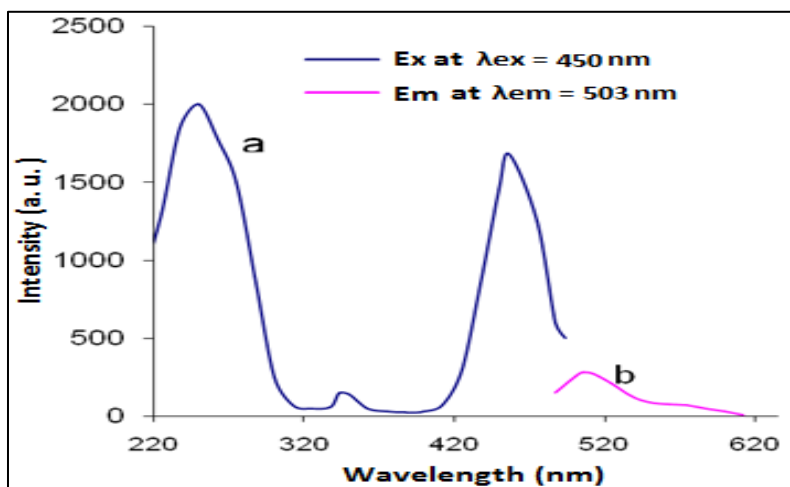**Figure 1.2A (i): PL Spectra of SrS:Eu for Excitation and Emission**

Figure 1.2B (i): PL Spectra of CaS:Ce (0.1%), (a) Excitation Spectra of CaS:Ce (0.1%) at λem=500nm (b) Emission Spectra of CaS:Ce(0.1%) at λex=450nm
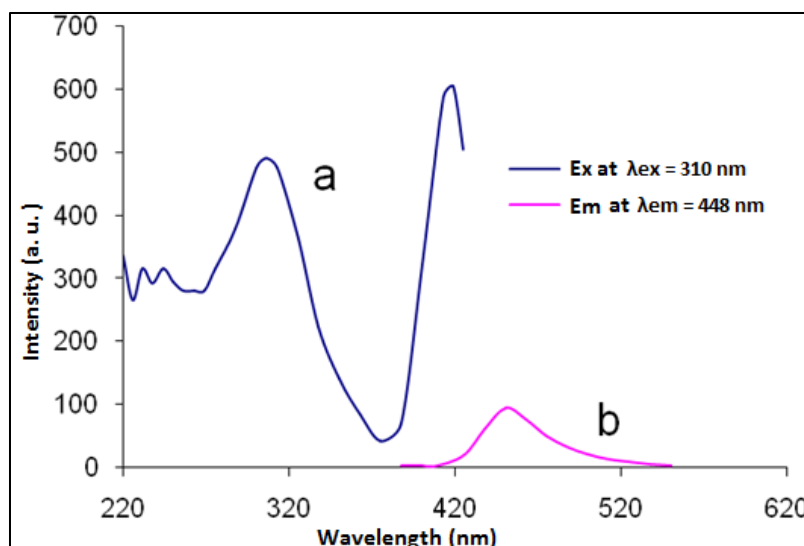

Figure 1.2B (ii): PL Spectra of CaS:Ce (0.2%), (a) Excitation Spectra of CaS:Ce (0.2%) at λem=503nm, (b) Emission Spectra of CaS:Ce (0.2%) at λex=450nm

Research Article

Figure 1.2B (iii): PL Spectra of CaS:Ce (0.5%), (a) Excitation Spectra of CaS:Ce (0.5%) at λem=503nm, (b) Emission Spectra of CaS:Ce (0.5%) at λex=450nm

Figure 1.2C (i): PL Spectra of CaS:Bi (0.1%), (a) Excitation Spectra of CaS:Bi (0.1%) atλem=448nm, (b) Emission Spectra of CaS:Bi (0.1%) at λex=310nm

Conclusion
In the present investigation we report sulfide based phosphor Eu^{2+} doped strontium sulfide and Ce^{3+} and Bi^{3+}doped calcium sulfide phosphor for solid state lighting. The synthesis of phosphors (chosen material to synthesize such phosphors are strontium sulfide and Calcium sulfide act as host), which can be excited in the blue/ near UV region i.e. between the range 360 nm to 390 nm and emits in the red, green or blue region. $SrSO_4$:Eu phosphors, CaS:Ce phosphors and CaS:Bi phosphors were prepared by recrystallization through sulfuric acid (Yamashita's method).
A Photoluminescence spectra were successfully recorded over fluorescence spectrophotometer in the range 220-700 showed intense red emission from $SrS:Eu^{2+}$; intense green emission from $CaS:Ce^{3+}$ whereas $CaS:Bi^{3+}$ exhibits intense blue emission and thus, helps in achieving safe disposal of burnt lamps causing minimization of environmental pollution, reduced by heating in reducing atmosphere provided by burning charcoal, minimization of stability problem (usually found under Hg discharge), solving problem of importing of phosphors by our country as we have developed reliable method for the synthesis of phosphors useful for solid state lighting.

Research Article

REFERENCES
Blasse G and Grabmeier BC (1994). *Luminescent Materials*, (Springer-Verlag, Berlin/Heidelberg, Germany).

Buchanan RA, Raid HF and Luster HH (1966). Infrared Absorption of Ce3+ in LaF3 and of CeF3. *Journal of Chemical Physics* **44** 4063.

Dorenbos P (2003). Energy of first $4f^7 – 4f^6 5d$ transition in Eu^{2+} doped compounds. *Journal of Luminescence* **104**(4) 239-302.

Fasol G and Nakamura S (2000). *The Blue Laser Diode: GaN Based Blue Light Emitters and Lasers*, 2nd edition, (Springer-Verlag Berlin Heidelberg, Berlin, Germany) 152.

Guo CF, Luan L, Xu Y, Gao F and Liang LF (2008). White Light–Generation Phosphor $Ba_2Ca(BO_3)_2 : Ce^{3+}, Mn^{2+}$ for Light-Emitting Diodes. *Journal of Electrochemical Society* **155**(11) 310-314.

Hill CGA (1984). CRT Phosphors, *SID Seminar Lecture Notes, S-6.2*.

Hoffman MV (1977). Emission characteristics. *The Journal of the Illuminating Engineering Society of North America* **6** 89.

Kawai H, Yokomo S, Abe T and Hoshine TJ (1981). Luminescent properties of ZnS:Ce, Li. *Journal of Luminescence* **24/25**(1) 163-166.

Kiss ZJ (1962). Optical Absorption of Sm2+ in CaF2 Type Crystals. Physical Review Letters **127** 718.

Lakshmanan AR (2008). *Luminescence and Display Phosphor: Phenomenon and Applications* 1st edition, (Nova Science Publishers, New York, USA) 101-110.

Li YQ, Delsing A, de With G and Hintzen HT (2005). Luminescence properties of Eu2+-activated alkaline-earth silicon-oxynitride MSi2O2-δN2+ 2/3δ (M= Ca, Sr, Ba): A promising class of novel LED conversion phosphors. *Chemistry of Materials* **17**(12) 3242-3248.

Li YQ, Hintzen HT and Buturi O (2007). Silicon-based oxynitride and nitride phosphors for white LEDs—A review. *Science and Technology of Advanced Materials* **76** 258-263.

Mandel G, Baumark P and Bunki FJ (1960). Ce(III) infra-red. *Chemical Physics* **33**(1) 192.

Wang JG, Jing XP, Yan CH and Lin JH (2005). Ca1− 2x Eu x Li x MoO4: A Novel Red Phosphor for Solid-State Lighting Based on a GaN LED. *Journal of the Electrochemical Society* **152**(3) 186-188.

Wang ZL, Quan ZW, Jia PY and Lin CK (2006). Handbook on the Physics and Chemistry of Rare Earths. *Chemistry of Materials* **18** 2030.

Wu JL, Gundiah G and Cheetham AK (2007). Structure-Property Correlations in Ce Doped Garnet Phosphors for Use in Solid State Lighting. *Chemical Physics Letters* **441** 250-254.

Xie RJ and Hirosaki N (2007). Silicon-based oxynitride and nitride phosphors for white LEDs - A review. *Science and Technology of Advanced Materials* **8**(7) 588-600.

Ye S, Wang CH and Jing XP (2009). Long wavelength extension of the excitation band of LiEuMo2O8 phosphor with Bi3+ doping. *Journal of the Electrochemical Society* **156** 121-124.

Yokomo S, Abe T and Hoshine T (1979). Phonon sidebands in Emission and Excitation Spectra for Ce3+ in CaS. *Journal of the Physical Society of Japan* **46** 351-352.

Zhang QF, Dandeneau CS, Zhou X and Cao G (2009). ZnO Nanostructures for Dye-Sensitized Solar Cells. *Advanced Materials* **21** 4087-4108.

Zhang QY and Huang XY (2010). Recent progress in quantum cutting phosphors. *Progress in Materials Science* **55**(5) 353-427.